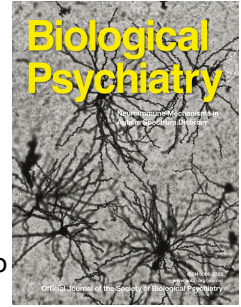


Journal Pre-proof



Glucocorticoid receptor-dependent astrocytes mediate stress vulnerability

Cheng-Lin Lu, Jing Ren, Jia-Wen Mo, Jun Fan, Fang Guo, Liang-Yu Chen, You-Lu Wen, Shu-Ji Li, Ying-Ying Fang, Zhao-Fa Wu, Yu-Long Li, Tian-Ming Gao, Xiong Cao

PII: S0006-3223(21)01833-3

DOI: <https://doi.org/10.1016/j.biopsych.2021.11.022>

Reference: BPS 14730

To appear in: *Biological Psychiatry*

Received Date: 9 July 2021

Revised Date: 4 November 2021

Accepted Date: 28 November 2021

Please cite this article as: Lu C.-L., Ren J., Mo J.-W., Fan J., Guo F., Chen L.-Y., Wen Y.-L., Li S.-J., Fang Y.-Y., Wu Z.-F., Li Y.-L., Gao T.-M. & Cao X., Glucocorticoid receptor-dependent astrocytes mediate stress vulnerability, *Biological Psychiatry* (2022), doi: <https://doi.org/10.1016/j.biopsych.2021.11.022>.

This is a PDF file of an article that has undergone enhancements after acceptance, such as the addition of a cover page and metadata, and formatting for readability, but it is not yet the definitive version of record. This version will undergo additional copyediting, typesetting and review before it is published in its final form, but we are providing this version to give early visibility of the article. Please note that, during the production process, errors may be discovered which could affect the content, and all legal disclaimers that apply to the journal pertain.

© 2021 Published by Elsevier Inc on behalf of Society of Biological Psychiatry.

1 **Glucocorticoid receptor-dependent astrocytes mediate stress**
2 **vulnerability**

3 Short Title: Astrocytes regulate depressive-like behaviors via GRs

4 Cheng-Lin Lu^{1#}, Jing Ren^{1#}, Jia-Wen Mo¹, Jun Fan¹, Fang Guo¹, Liang-Yu Chen¹, You-Lu
5 Wen³, Shu-Ji Li¹, Ying-Ying Fang¹, Zhao-Fa Wu⁴, Yu-Long Li⁴, Tian-Ming Gao¹, Xiong
6 Cao^{1,2*}

7
8 1. Key Laboratory of Mental Health of the Ministry of Education, Guangdong-Hong
9 Kong-Macao Greater Bay Area Center for Brain Science and Brain-Inspired Intelligence,
10 Guangdong Province Key Laboratory of Psychiatric Disorders, Department of
11 Neurobiology, School of Basic Medical Sciences, Southern Medical University,
12 Guangzhou 510515, P. R. China.

13 2. Microbiome Medicine Center, Department of Laboratory Medicine, Zhujiang Hospital,
14 Southern Medical University, Guangzhou, Guangdong 510515, P. R. China.

15 3. Department of Psychology and Behavior, Guangdong 999 Brain Hospital, Guangzhou
16 510510, China

17 4. State Key Laboratory of Membrane Biology, Peking University School of Life Sciences,
18 Beijing 100871, China

19 # Cheng-Lin Lu and Jing Ren contributed equally to this work.

20 *Address correspondence to Xiong Cao, Ph.D., at caoxiong@smu.edu.cn

21 **ABSTRACT**

22 **BACKGROUND:** Major depressive disorder (MDD) is a devastating psychiatric illness
23 that affects approximately 17% of the population worldwide. Astrocyte dysfunction has
24 been implicated in the pathophysiology of MDD. Traumatic experiences and stress
25 contribute to the onset of MDD, but how astrocytes respond to stress is poorly
26 understood.

27 **METHODS:** Using western blot analysis, we identified stress vulnerability was associated
28 with reduced astrocytic glucocorticoid receptor (GR) expression in mouse models of
29 depression. We further investigated the functions of astrocytic GRs in regulating
30 depression and the underlying mechanisms by using a combination of behavioral studies,
31 fiber photometry, biochemical experiments, and RNA-sequencing methods.

32 **RESULTS:** GRs in astrocytes were more sensitive to stress than those in neurons. The
33 GR absence in astrocytes induced depressive-like behaviors, whereas restoring astrocytic
34 GR expression in the medial prefrontal cortex (mPFC) prevented the depressive-like
35 phenotype. Furthermore, we found that GRs in the mPFC affected astrocytic Ca^{2+} activity
36 and dynamic adenosine 5'-triphosphate (ATP) release in response to stress.
37 RNA-sequencing of astrocytes isolated from GR deletion mice identified the PI3K-AKT
38 signaling pathway, which was required for astrocytic GR-mediated ATP release.

39 **CONCLUSIONS:** These findings reveal that astrocytic GRs play an important role in the
40 stress response and that the reduced astrocytic GR expression in the stressed subject
41 decreases ATP release to mediate stress vulnerability.

42 **Keywords:** Depression; Astrocyte; GR; ATP; Stress vulnerability; PI3K

43 **BACKGROUND**

44 Major depressive disorder (MDD) is the most prevalent psychiatric disease, with
45 approximately 17% of the world's population affected by MDD in their lifetime (1). The
46 morbidity, mortality, and socioeconomic burden associated with MDD make it a
47 devastating psychiatric illness. Astrocytes, the majority cell type among glial cells, execute
48 a variety of essential functions, including their contribution to the blood-brain barrier,
49 synaptogenesis, ion homeostasis, neurotransmitter buffering, and the secretion of
50 neuroactive agents (2, 3). Accumulated evidence indicates that dysfunction of astrocytes
51 is involved in the pathophysiology of MDD (4, 5). Evidence from human subjects and
52 animal models of depression has shown that morphological and numerical changes in glia
53 in the prefrontal area (6, 7) and pharmacologic glial ablation in the mPFC induce
54 depressive-like behaviors (8). Astrocytes are known to release ATP in the mPFC, which
55 are vital in the induction of depressive symptoms and antidepressant responses (9, 10).
56 However, how astrocytes respond to stress and contribute to the pathogenesis of
57 depression remains unclear.

58 Traumatic experiences and social stress, contributing to the onset of MDD, trigger
59 stress responses including activation of the hypothalamic-pituitary-adrenal (HPA) axis and
60 the release of glucocorticoid hormones (11-13). Glucocorticoid hormones activate GRs,
61 which are expressed ubiquitously in the brain, during the stress response (11, 12, 14).
62 GRs in neurons have been shown to modulate depressive-like behaviors in animal studies
63 (15-19). However, the GR expression is markedly higher in astrocytes than in neurons in
64 the brain (20). Astrocytes are the key components of the brain-blood barrier (21), and

65 glucocorticoids already in the blood activate astrocytic GRs earlier than neuronal GRs in
66 the brain. However, whether astrocytic GRs respond to stress and modulate
67 depressive-like behaviors remains largely unexplored.

68 Here, we showed that stress vulnerability was associated with reduced astrocytic GR
69 expression. Astrocyte-specific knockout of *Nr3c1* (encoding GRs) was sufficient to induce
70 depressive-like behaviors, which was rescued by restoring GRs in astrocytes in the mPFC.
71 We then showed that astrocytic GRs in the mPFC modulated depressive-like phenotypes.
72 Moreover, the GR absence in astrocytes decreased the Ca^{2+} activity and ATP release in
73 the mPFC. RNA sequencing indicated that the GR regulated ATP release from astrocytes
74 via the PI3K-AKT signaling pathway. Our study suggests that astrocytic GRs buffer the
75 consequences of stress and that the activation of astrocytic GRs in the stressed subject
76 seems to release a putative messenger to alert the body to stress.

77

78 **METHODS AND MATERIALS**

79 **Animals**

80 The *Nr3c1^{loxP/loxP}* mice were purchased from the Jackson Laboratory (cat# 021021). The
81 *Fgfr3-iCreER^{T2}* mice (C57BL/6J background) were generously provided by William D.
82 Richardson (University College London, London, UK). All animal experiments were
83 approved by the Southern Medical University Animal Ethics Committee.

84 Detailed methods and materials regarding additional animals, reagents, virus injections,
85 behavioral tests, and biochemical experiments are provided in the Supplement
86 Information.

87 **RESULTS**88 **The GR in astrocytes is more sensitive to stress than that in neurons**

89 To confirm that the aberrant expression of GRs is universal in depression (22, 23), we first
90 used chronic social defeat stress (CSDS), a well-established model of depression that
91 mimics several psychopathological dimensions of depression (24). In the 10-days CSDS
92 protocol, eight-week-old male C57BL/6J mice were exposed to a physically aggressive
93 CD-1 mouse (10 min d⁻¹) for social defeat (Figure 1A). CSDS induced a social avoidance
94 behavior in a subset of mice as assessed with the social interaction (SI), termed
95 stress-susceptible (Sus). Defeated mice that did not display social avoidance were
96 considered resilient (Res; Figure 1B). Then, we detected the GR protein level in the
97 mPFC, a candidate site for impaired function in depression (9, 10). Western blot analysis
98 showed that the GR protein was significantly reduced in the mPFC of Sus mice compared
99 to control mice (Figure 1C). Additionally, the GR protein level was positively correlated
100 with the social interaction (SI) ratio in the social interaction test (Figure 1D). Meanwhile,
101 the adult mice were subjected to 3-days subthreshold social defeat stress (SSDS), which
102 did not induce social avoidance behaviors and a reduction of total GR expression in the
103 mPFC (Figure S2A, B). We next evaluated whether significant changes in GR expression
104 were present in which depression was induced by treatment with lipopolysaccharide (LPS)
105 (25). Ten days of LPS injection (0.5 mg kg⁻¹ per day, intraperitoneal (i.p.)) in
106 eight-week-old C57BL/6J mice was sufficient to cause depressive-like behaviors in the
107 forced swim test (FST; Figure 1 E, F) and sucrose preference test (25). Mice with
108 LPS-induced depression also showed a significant decrease in the GR protein level in the

109 mPFC (Figure 1G), and the GR protein level was negatively correlated with immobility
110 time in the FST (Figure 1H).

111 Neurons and astrocytes are two major cell types in the adult brain. To determine which
112 subtype of cells is more sensitive to stress, we first detected GR expression in neurons
113 and astrocytes. We found that GRs were present in most astrocytes and neurons (Figure
114 S1A-E). Western blot analysis showed that the GR protein level was higher in cultured
115 astrocytes than in neurons (Figure S1F), consistent with previous reports (20). We then
116 detected the GR protein level in cultured astrocytes and neurons during the stress
117 response. A reduction of GR protein level was observed in cultured astrocytes treated with
118 LPS ($1 \mu\text{g ml}^{-1}$) at 8 d in vitro (DIV8), and neurons (DIV14) showed no difference in the GR
119 protein level upon LPS ($1 \mu\text{g ml}^{-1}$) treatment (Figure 1I). Stress activates the HPA axis and
120 enhances the release of glucocorticoid hormones, which activate GRs in the brain (13).
121 Then, we directly treated cultured astrocytes (DIV8) and neurons (DIV14) with GR agonist
122 dexamethasone (DXMS) to mimic the stress condition. The results showed that the GR
123 protein level was downregulated in astrocytes exposed to $1 \mu\text{M}$ and $5 \mu\text{M}$ DXMS for 6 h,
124 but no difference was observed in neurons (Figure 1J). We also found that the GR protein
125 level was downregulated in astrocytes exposed to DXMS ($1 \mu\text{M}$) for 24 h and 48 h.
126 Meanwhile, the treatment of neurons with DXMS ($1 \mu\text{M}$) for 48 h induced the
127 downregulation of the GR protein (Figure 1K). To determine the levels of astrocytic GRs of
128 mice under stress, adult mice were subjected to SSDS or CSDS. After SSDS or CSDS,
129 the mPFC slices of mice were stained to visualize GRs with S100 β (a marker of
130 astrocytes) and NeuN (a marker of neurons). Immunostaining and quantification revealed

131 that the GR protein level was markedly decreased in astrocytes in the mPFC after SSDS
132 (Figure 1L), but no difference was observed in neurons (Figure 1M). After CSDS, GRs
133 were decreased in both astrocytes and neurons in the mPFC of Sus mice (Figure S2C, D).
134 Then, we isolated astrocytes from the mPFC by fluorescence-activated cell sorting (FACS)
135 after the CSDS paradigm. Simple western blot analysis also showed that astrocytic GRs
136 were decreased in the mPFC of Sus mice compared with control mice (Figure S2E).
137 Taken together, these results suggest that astrocytes contribute to the stress-induced
138 reduction of GRs, and GRs in astrocytes are more sensitive to stress than those in
139 neurons in the mPFC.

140 **Astrocyte-specific knockout of *Nr3c1* induces depressive- and anxiety-like** 141 **behaviors**

142 To evaluate the role of astrocytic GRs in depression, we generated an astrocyte-specific
143 GR deletion mouse line, *Fgfr3-iCreER^{T2}; Nr3c1^{loxP/loxP}*, for behavioral studies (Figure 2A).
144 To obtain this model, we crossed mice with the floxed *Nr3c1* allele with the *Fgfr3-iCreER^{T2}*
145 mouse line, allowing selective *Nr3c1* deletion in astrocytes via tamoxifen-inducible Cre
146 recombination (Figure 2A and Figure S3A). To examine the efficiency and specificity of
147 GR deletion in astrocytes, brain tissues were collected from adult mice and studied 28
148 days after the first tamoxifen injection. *Fgfr3-iCreER^{T2}; Nr3c1^{loxP/loxP}* (cKO) and littermate
149 control (Ctrl) mice exhibited normal growth rates, body weights and brain sizes (Figure S3
150 B-D). No apparent differences in brain structure, astrocytes, and neurons density were
151 observed between the cKO and Ctrl mice (Figure S3 E-G). Immunostaining revealed that
152 GRs were attenuated in GFAP-positive astrocytes (Figure S3H) and not changed in

153 NeuN-positive neurons (Figure S3I) in the mPFC of cKO mice compared to Ctrl mice. In
154 addition, flow cytometry analysis showed a more than 50% reduction of astrocytic GR
155 expression in cKO mice compared to Ctrl mice (Figure 2 B, C, and Figure S4A).

156 For behavioral studies, all mice were treated with tamoxifen for 5 continuous days.
157 Allowed 28 days recovery to induced downregulation of GRs, mice were then subjected to
158 a battery of depression-related behavioral tests. In the FST, the duration of immobility was
159 increased in cKO mice compared with Ctrl mice (Figure 2D). To assess whether a loss of
160 GRs increases stress vulnerability, we then subjected mice to the SSDS experiment (26),
161 in which no difference in interaction zone time when the social target was present was
162 observed between defeated and undefeated Ctrl mice (Figure 2E). However, defeated
163 cKO mice displayed greater social avoidance than undefeated cKO mice (Figure 2E). No
164 difference was observed in sucrose preference (Figure S5A) and tail suspension test (TST;
165 Figure S5B). Next, mice were subjected to anxiety-related behavioral tests. The results
166 showed that cKO mice spent less time in the open arm in the elevated-plus maze (EPM;
167 Figure 2F) and stayed longer in the dark box in the light-dark box (LD box; Figure 2G)
168 compared to Ctrl mice. cKO mice also displayed reduced general locomotion in the open
169 field test (OFT; Figure 2 H, I), but no difference in motor coordination was observed in the
170 rotarod test (Figure 2J). These observations indicate that the GR absence in astrocytes
171 induces depressive- and anxiety-like behaviors in adult mice.

172

173 **Astrocytic GR dysfunction in the mPFC displays depressive-like phenotypes**

174 To determine whether the selective knockout of astrocytic GRs in the mPFC would induce

175 depressive-like behaviors, we bilaterally injected AAV-GFAP-Cre or AAV-GFAP-EYFP
176 viruses into the mPFC of *Nr3c1^{loxP/loxP}* mice for behavioral studies (Figure 3A). Confocal
177 imaging showed that the GFAP-Cre virus was specifically expressed on astrocytes in the
178 mPFC (Figure 3B and Figure S6A), and western blot analysis showed that the GR protein
179 level was decreased in the knockout mice (Figure 3C). We next assayed depressive-like
180 phenotypes and found that mice infected with the AAV-GFAP-Cre virus displayed
181 depressive-like behaviors, including increased immobility time in the FST (Figure 3D) and
182 social avoidance after the SSDS (Figure 3E and Figure S6B). However, the
183 AAV-GFAP-Cre virus had no effect on anxiety-related behaviors or general locomotion
184 (Figure 3F-H).

185 To determine whether the restoration of astrocytic GRs in the mPFC would be sufficient
186 to reverse the depressive-like behaviors caused by astrocytic GR knockout, we bilaterally
187 injected AAV-DIO-Nr3c1 or control viruses into the mPFC of cKO and Ctrl mice. Confocal
188 imaging showed that the virus was expressed on mPFC astrocytes (Figure 3I) and
189 western blot analysis showed that the GR was overexpressed in the mPFC in the mice
190 infected with the AAV-DIO-Nr3c1 virus (Figure S6C). Then, all mice were subjected to the
191 SI test to assess the social avoidance behavior before and after the SSDS. After the
192 SSDS paradigm, cKO mice infected with the control virus also displayed social avoidance
193 behaviors in the SI test (Figure 3J and Figure S6D). Interestingly, the social avoidance
194 behavior in cKO mice was reversed by the restoration of GRs in astrocytes in the mPFC
195 (Figure 3J and Figure S6D). In parallel experiments, the GR overexpression had no
196 detectable effect on the social avoidance behavior of control mice before and after the

197 SSDS (Figure 3J and Figure S6D). Additionally, no difference in locomotion activity in the
198 OFT was observed (Figure 3 K, L). Taken together, these results indicate that the
199 impairment of astrocytic GRs in the mPFC is sufficient to induce depressive-like
200 behaviors.

201

202 **The GR deletion causes dysfunction of astrocytic Ca²⁺ activity in the mPFC**

203 Astrocyte Ca²⁺ signaling is important for intercellular communication to regulate
204 physiological function (27-29). Therefore, we assessed astrocytic function in the mPFC of
205 cKO and Ctrl mice. We injected the AAV-GFAP-GCaMP6s virus, which preferentially
206 targets astrocytes due to the GFAP promoter, into the mPFC, and optical fibers were
207 implanted above the infected cells to carry out fiber photometry recordings (Figure 4A, B).
208 Confocal images and quantification showed that more than 90% of Gcamp6s were
209 expressed in GFAP-positive astrocytes (Figure S7A-C). Fluorescence signals from
210 astrocytes in the mPFC were measured two weeks after injection while mice in a
211 protective wire-mesh enclosure were attacked by an aggressor mouse in the forced
212 interaction test (FIT; Figure 4A, B) (30, 31). Before the SSDS paradigm, the astrocytic
213 Ca²⁺ signals of cKO mice were increased during attack periods compared to non-attack
214 periods and similar to those of control mice (Figure 4 C-E). After 3 days of SSDS, control
215 mice also showed a large increase in Ca²⁺ signaling during an attack. Notably, the
216 magnitude of this increase was attenuated in cKO mice (Figure 4 C-E). These results
217 suggest that Ca²⁺ activity is reduced in response to stress after the deletion of astrocytic
218 GRs and that GRs in astrocytes may affect the Ca²⁺-evoked release of neurotransmitters.

219 GRs modulate astrocytic ATP release in the mPFC

220 To explore how astrocytic GRs in the mPFC modulate depressive-like behaviors, we first
221 detected plasma corticosterone levels. No difference in plasma corticosterone was
222 observed between cKO and Ctrl mice under basal conditions or after an additional acute
223 social defeat episode (Figure 5A). We next analyzed the amounts of neurotransmitters
224 and inflammatory cytokines, known to be secreted by astrocytes (10, 32, 33), in the PFC
225 of cKO and Ctrl mice (Figure 5B and Figure S8A). Notably, the concentration of ATP was
226 lower in the artificial cerebral spinal fluid (ACSF) from PFC slices derived from cKO mice
227 (Figure 5B). Furthermore, in vivo microdialysis in freely moving mice demonstrated that
228 ATP concentrations in the interstitial fluid of the mPFC were significantly decreased in
229 cKO mice compared to Ctrl mice (Figure 5C), indicating that GRs seem to regulate
230 astrocytic ATP release.

231 To determine whether GRs regulate ATP release from astrocytes, we first employed
232 pharmacological approaches. The application of DXMS increased ATP accumulation in
233 the medium collected from cultured astrocytes 4 h after the treatment (Figure 5D). The
234 ability of GRs to enhance ATP release from astrocytes was further confirmed using
235 virus-mediated conditional knockout of GRs in cultured astrocytes isolated from
236 *Nr3c1^{loxP/loxP}* mice. The results showed that cultured astrocytes infected with
237 pLenti-EGFP-Cre induced downregulation of the GR protein (Figure S8B-C). DXMS
238 treatment also increased ATP release from astrocytes infected with the control virus, and
239 the effect of DXMS in enhancing ATP levels was blocked by the knockout of GRs (Figure
240 5E).

241 Furthermore, to detect extracellular ATP dynamics in the mPFC in vivo at a high
242 temporal resolution and with high specificity and sensitivity, we virally expressed an ATP
243 sensor (AAV-GfaABC1D-ATP1.0) in astrocytes of the mPFC of cKO and Ctrl mice, and
244 the amount of extracellular ATP was indicated by the intensity of fluorescence produced
245 by green fluorescent protein (GFP). Two weeks after injection of the virus, fluorescence
246 signals from astrocytes while mice were attacked by an aggressor mouse during the FIT
247 were recorded using fiber photometry (Figure 5F, G). Before SSDS, fluorescence signals
248 in both cKO and Ctrl mice increased when the mice were attacked by a CD1 aggressor
249 (Figure 5 H-I). No significant difference in peak fluorescence signal was observed
250 between the two groups (Figure 5J). After 3 days of SSDS, control mice also displayed a
251 large increase in fluorescence during attack periods (Figure 5 H-I). However, this effect
252 was reduced in cKO mice (Figure 5J).

253 Next, to define the role of ATP in the depressive-like behaviors caused by astrocytic
254 GR deletion, we directly administered ATP to cKO mice (Figure 5K). Following the i.p.
255 injection of ATP (125 mg per kg body weight) into the cKO mice, we observed that ATP
256 treatment reduced the immobility time of the cKO mice in the FST (Figure 5L). No
257 difference in locomotion activity in the OFT was observed (Figure S8D, E). Taken together,
258 these results demonstrate that ATP release is impaired after the deletion of astrocytic GRs
259 and that impairment of ATP release contributes to the depressive-like behaviors induced
260 by astrocyte-specific loss of GRs.

261

262 **GRs regulate ATP release from astrocytes mediated by the PI3K-AKT signaling**

263 **pathway**

264 The GR is a constitutively expressed transcriptional regulatory factor (TRF) that controls
265 many distinct gene networks (34). To explore how GRs modulate astrocytic ATP release,
266 we examined the mRNA expression profiles of astrocytes isolated from the mPFC of cKO
267 and Ctrl mice with FACS by RNA sequencing (RNA-seq) analysis. A volcano plot showed
268 that 389 genes were upregulated, while 89 genes were downregulated in cKO mice
269 (Figure 6A). The overall expression profiles of the Ctrl and cKO groups obtained after
270 hierarchical cluster analysis showed clear separation of the differentially expressed genes
271 (DEGs; Figure 6B). Kyoto Encyclopedia of Genes and Genomes (KEGG) pathway
272 analysis indicated that the PI3K-AKT signaling pathway was significantly enriched within
273 the dataset (Figure 6C).

274 To directly test whether the PI3K-AKT signaling pathway is involved in GR-dependent
275 ATP release from astrocytes, we employed pharmacological approaches. Western blot
276 analysis showed that DXMS significantly increased the phosphorylation of PI3K and AKT
277 in cultured astrocytes (Figure 6D). LY29004, a selective PI3K inhibitor, attenuated
278 astrocytic ATP release caused by DXMS (Figure 6E). These results indicate that
279 GR-dependent ATP release from astrocytes was mediated by the PI3K-AKT signaling
280 pathway. PI3K has been reported to regulate intracellular vesicular traffic and
281 homeostasis of the lysosome (35). Lysosome exocytosis is shown to be responsible for
282 ATP release in astrocytes (36). Therefore, we then investigated the effects of
283 glycyphenylalanine 2-naphthylamide (GPN) that selectively induces lysosome
284 osmodialysis on the ATP release in cultured astrocytes (36). The results revealed that the

285 DXMS-induced enhancement in astrocytic ATP release was decreased by the treatment
286 with 200 μ M GPN (Figure 6F). To evaluate the effect of PI3K activation on lysosomes, we
287 treated astrocytes with 740 Y-P (PI3K agonist; 50 μ g ml⁻¹) for 4 h (37, 38), and then
288 analyzed the astrocytic lysosomal compartment with LysoTracker, a weakly basic amine
289 fluorescent probe that accumulates in acidic compartments such as lysosomes.
290 Astrocytes incubated with LysoTracker were imaged and the mean fluorescence intensity
291 of fluorescence-positive lysosomes was quantified. We found that mean fluorescence
292 intensity was decreased in astrocytes treated with 740 Y-P compared to control astrocytes
293 (Figure 6G, H). To examine whether PI3K activation in astrocytes affects lysosome
294 numbers or size, astrocytes were stained with Lamp1, a lysosomal marker, after treatment
295 with 740 Y-P for 4 h. The results showed that PI3K activation significantly increased the
296 number of lysosomes compared to control astrocytes (Figure 6I, J). No difference in
297 distributions of the lysosomal size was observed between these two groups (Figure 6K).
298 Taken together, these findings suggest that GR-dependent ATP release from astrocytes
299 through lysosome exocytosis requires activation of the PI3K-AKT signaling pathway.

300

301 **DISCUSSION**

302 Overall, we found that chronic stress induced a reduction in GRs in astrocytes.
303 Furthermore, astrocyte-specific knockout of GRs was found to be sufficient to induce
304 depressive-like behaviors. The reduction in astrocytic GRs decreased ATP release, which
305 was mediated by the PI3K-AKT signaling pathway. We previously reported that
306 astrocyte-derived ATP modulated depressive-like behaviors and P2X2 receptors in the

307 mPFC were required for the antidepressant-like effect of ATP (10). Together, our study
308 suggests that temporal elevations in glucocorticoid levels preferentially activated
309 astrocytic GRs, thereby enhancing extracellular ATP release through lysosome
310 exocytosis. ATP released from astrocytes binds to purinergic receptors on neurons.
311 Chronic stress induced a reduction of astrocytic GRs in the mPFC, which consequently
312 caused decreased ATP released from astrocytes to regulate depressive-like behaviors
313 (Figure 6L).

314 Neurochemical evidence suggests that chronic stress enhances the excitability of the
315 HPA, which drives the release of glucocorticoid hormones into the blood (16, 18, 39, 40).
316 Glucocorticoid hormones in the blood can be transported into the brain through the
317 blood-brain barrier. Previous studies have reported that hyperactivity of the HPA axis is
318 observed in the majority of patients with depression (41), and up to 40–60% of depressed
319 patients experience hypercortisolemia (17). Pathological activation of the prefrontal
320 cortical GRs by chronic stress negatively impacts the GR expression, suggesting the loss
321 of prefrontal feedback control (22, 42). Previous studies and our data indicated that the
322 GR expression in astrocytes was higher than that in neurons in the brain (20). And chronic
323 stress induced a reduction of astrocytic GRs in the mPFC. Therefore, astrocytic GRs may
324 contribute to glucocorticoid hormones feedback control.

325 The GR expression is detected in most mouse cell subsets, including astrocytes,
326 neurons, microglia, endothelial cells, and oligodendrocytes (20). Previous studies have
327 shown that GRs in neurons modulate depressive-like behaviors (15-17, 43). However, the
328 effects of GRs in other cell subtypes in depression, such as astrocytes, have been poorly

329 explored. In a previous study, astrocyte-specific elimination of GRs impaired contextual
330 fear memory but did not elicit depressive-like symptoms in TST and sucrose preference
331 (44). In our study, we found astrocyte-specific knockout of the GRs induced
332 depressive-like behaviors in FST and SSDS. Similarly, we also did not find cKO mice
333 displayed depressive-like behaviors in TST and sucrose preference (Figure S5A, B).
334 Given the multifactorial nature and heterogeneity of major depression, different animal
335 depression models can only mimic some of the characteristics of depression (45).
336 Besides, knockdown of the astrocytic GRs in the central nucleus of the amygdala
337 diminishes conditioned fear expression and anxiety (46). In our study, we found global
338 astrocyte-specific knockout of GRs induced anxiety-like behaviors. However, knockdown
339 of the astrocytic GRs in the mPFC did not induce anxiety-like behavior. Therefore,
340 astrocytic GRs in other brain regions may play a role in fear memory and anxiety. In
341 addition, our experiments indicated that chronic stress induced a reduction of the GR
342 expression in astrocytes and that astrocytes were more sensitive to the stress response
343 than neurons. In the present study, we provide direct evidence that astrocytes are likely to
344 respond to stress before neurons to protect neurons from high concentrations of
345 glucocorticoid hormones. Astrocytic GRs seem to be a necessary molecule to the onset of
346 depression. However, the role of GRs in other cell subtypes in response to stress and the
347 relationships among these cells in MDD require further determination.

348 Previous studies have shown that exposure to stress rapidly increases the release of
349 neurotransmitters from synapses, which leads to the Ca^{2+} -dependent exocytosis of ATP
350 from astrocytes (32, 33). ATP and its metabolite, adenosine, activate disparate

351 presynaptic purinergic receptor subtypes to regulate synaptic efficacy (32, 47). However,
352 our results suggest that GRs in astrocytes activated by circulating corticosterone promote
353 ATP release, indicating that stress-induced circulating corticosterone directly modulates
354 astrocytic ATP release. Previous studies have also proven that glucocorticoid hormones
355 regulate ATP release from spinal astrocytes (48). Several possible pathways have been
356 shown to be responsible for ATP release in astrocytes including vesicular exocytosis and
357 non-exocytosis (49). Here, we show that GR-dependent ATP release from astrocytes
358 through lysosome exocytosis requires activation of the PI3K-AKT signaling pathway.
359 Though the PI3K has been reported to regulate intracellular vesicular traffic and
360 homeostasis of the lysosome (35), the relationship between lysosome exocytosis and the
361 PI3K-AKT signaling pathway under stress needs to be further determined.

362 Moreover, we found that a reduction in astrocytic GRs results in increased
363 inflammatory factors (Figure S8A). Given that neuroinflammation is tightly associated with
364 the onset of depression (25, 50, 51), it seems likely that astrocyte neuroinflammatory
365 mechanisms also play a role in depression.

366 In summary, our findings demonstrate a critical role for astrocytic GRs as the
367 regulator of depressive-like behaviors and establish the priority of astrocytes in response
368 to stress.

369

370 **ACKNOWLEDGMENTS AND DISCLOSURES**

371 We thank William D. Richardson (University College London, London, UK) for providing
372 the *Fgfr3-iCreER^{T2}* mice. We also thank Xiao-Wen Li, Li-Rong Sun, and Ting Guo

373 (Southern Medical University) for their technical support. This work was supported by the
374 National Natural Science Foundation of China (31771187), the Guangzhou Science and
375 Technology Project (201904020039, 202007030013), the National Program for Support of
376 Top-notch Young Professionals, The Key Area Research and Development Program of
377 Guangdong Province (2018B030334001, 2018B030340001), and the Program for
378 Changjiang Scholars and Innovative Research Team in University (IRT_16R37).

379 The authors report no biomedical financial interests or potential conflicts of interest.

380

381 **AUTHOR CONTRIBUTIONS**

382 X.C. and C.-L.L. designed the study and wrote the paper. X.C. J.R. and C.-L.L. analyzed
383 the data. J.R. and C.-L.L. performed most of the experiments. J.R. and C.-L.L. performed
384 behavioral experiments and stereotactic injection with the help of Y.-Y.F. and F.G.
385 performed the Western blotting. J.-W.M. and Y.-L.W. performed the FACS. J.F. performed
386 the ATP assays. J.R. and S.-J. L. were responsible for cell culture. L.-Y.C. carried out
387 genotyping. F.-Z. W. and Y.-L. L. provided the GRAB_{ATP1.0} virus. T.-M. G. reviewed and
388 edited the manuscript. X.C. supervised all phases of the project.

389

390 **REFERENCES**

- 391 1. World Health Organization (2017): Depression and other common mental disorders:
392 global health estimates. [https://app.mhpss.net/resource/depression-and-other-common-](https://app.mhpss.net/resource/depression-and-other-common-mental-disorders-global-health-estimates)
393 [mental-disorders-global-health-estimates](https://app.mhpss.net/resource/depression-and-other-common-mental-disorders-global-health-estimates).
- 394 2. Khakh BS, Sofroniew MV (2015): Diversity of astrocyte functions and phenotypes in

- 395 neural circuits. *Nature neuroscience*. 18:942-952.
- 396 3. Nagai J, Yu X, Papouin T, Cheong E, Freeman MR, Monk KR, et al. (2021):
397 Behaviorally consequential astrocytic regulation of neural circuits. *Neuron*. 109:576-596.
- 398 4. Banasr M, Dwyer JM, Duman RS (2011): Cell atrophy and loss in depression:
399 reversal by antidepressant treatment. *Current opinion in cell biology*. 23:730-737.
- 400 5. Torres-Platas SG, Nagy C, Wakid M, Turecki G, Mechawar N (2015): Glial fibrillary
401 acidic protein is differentially expressed across cortical and subcortical regions in healthy
402 brains and downregulated in the thalamus and caudate nucleus of depressed suicides.
403 *Molecular Psychiatry*. 21:509-515.
- 404 6. Ongur D, Drevets WC, Price JL (1998): Glial reduction in the subgenual prefrontal
405 cortex in mood disorders. *Proc Natl Acad Sci U S A*. 95:13290-13295.
- 406 7. Miguel-Hidalgo JJ, Baucom C, Dilley G, Overholser JC, Meltzer HY, Stockmeier CA,
407 et al. (2000): Glial fibrillary acidic protein immunoreactivity in the prefrontal cortex
408 distinguishes younger from older adults in major depressive disorder. *Biological psychiatry*.
409 48:861-873.
- 410 8. Banasr M, Duman RS (2008): Glial loss in the prefrontal cortex is sufficient to induce
411 depressive-like behaviors. *Biological psychiatry*. 64:863-870.
- 412 9. Xiong W, Cao X, Zeng Y, Qin X, Zhu M, Ren J, et al. (2019): Astrocytic
413 Epoxyeicosatrienoic Acid Signaling in the Medial Prefrontal Cortex Modulates
414 Depressive-like Behaviors. *J Neurosci*. 39:4606-4623.
- 415 10. Cao X, Li LP, Wang Q, Wu Q, Hu HH, Zhang M, et al. (2013): Astrocyte-derived ATP
416 modulates depressive-like behaviors. *Nature medicine*. 19:773-777.

- 417 11. Huhman KL (2006): Social conflict models: can they inform us about human
418 psychopathology? *Horm Behav.* 50:640-646.
- 419 12. Kelleher I, Harley M, Lynch F, Arseneault L, Fitzpatrick C, Cannon M (2008):
420 Associations between childhood trauma, bullying and psychotic symptoms among a
421 school-based adolescent sample. *Br J Psychiatry.* 193:378-382.
- 422 13. Oakley RH, Cidlowski JA (2013): The biology of the glucocorticoid receptor: new
423 signaling mechanisms in health and disease. *J Allergy Clin Immunol.* 132:1033-1044.
- 424 14. de Kloet ER, Joels M, Holsboer F (2005): Stress and the brain: from adaptation to
425 disease. *Nature reviews Neuroscience.* 6:463-475.
- 426 15. Boyle MP, Brewer JA, Funatsu M, Wozniak DF, Tsien JZ, Izumi Y, et al. (2005):
427 Acquired deficit of forebrain glucocorticoid receptor produces depression-like changes in
428 adrenal axis regulation and behavior. *Proc Natl Acad Sci U S A.* 102:473-478.
- 429 16. Jacobson L (2014): Forebrain glucocorticoid receptor gene deletion attenuates
430 behavioral changes and antidepressant responsiveness during chronic stress. *Brain Res.*
431 1583:109-121.
- 432 17. Keller J, Gomez R, Williams G, Lembke A, Lazzeroni L, Murphy GM, Jr., et al. (2017):
433 HPA axis in major depression: cortisol, clinical symptomatology and genetic variation
434 predict cognition. *Mol Psychiatry.* 22:527-536.
- 435 18. Arnett MG, Muglia LM, Laryea G, Muglia LJ (2016): Genetic Approaches to
436 Hypothalamic-Pituitary-Adrenal Axis Regulation. *Neuropsychopharmacology : official
437 publication of the American College of Neuropsychopharmacology.* 41:245-260.
- 438 19. Wei Q, Lu XY, Liu L, Schafer G, Shieh KR, Burke S, et al. (2004): Glucocorticoid

- 439 receptor overexpression in forebrain: a mouse model of increased emotional lability. *Proc*
440 *Natl Acad Sci U S A*. 101:11851-11856.
- 441 20. Zhang Y, Chen K, Sloan SA, Bennett ML, Scholze AR, O'Keeffe S, et al. (2014): An
442 RNA-sequencing transcriptome and splicing database of glia, neurons, and vascular cells
443 of the cerebral cortex. *J Neurosci*. 34:11929-11947.
- 444 21. Abbott NJ, Ronnback L, Hansson E (2006): Astrocyte-endothelial interactions at the
445 blood-brain barrier. *Nature Reviews Neuroscience*. 7:41-53.
- 446 22. Mizoguchi K, Ishige A, Aburada M, Tabira T (2003): Chronic stress attenuates
447 glucocorticoid negative feedback: involvement of the prefrontal cortex and hippocampus.
448 *Neuroscience*. 119:887-897.
- 449 23. Guidotti G, Calabrese F, Anacker C, Racagni G, Pariante CM, Riva MA (2013):
450 Glucocorticoid receptor and FKBP5 expression is altered following exposure to chronic
451 stress: modulation by antidepressant treatment. *Neuropsychopharmacology : official*
452 *publication of the American College of Neuropsychopharmacology*. 38:616-627.
- 453 24. Golden SA, Covington HE, 3rd, Berton O, Russo SJ (2011): A standardized protocol
454 for repeated social defeat stress in mice. *Nature protocols*. 6:1183-1191.
- 455 25. Leng L, Zhuang K, Liu Z, Huang C, Gao Y, Chen G, et al. (2018): Menin Deficiency
456 Leads to Depressive-like Behaviors in Mice by Modulating Astrocyte-Mediated
457 Neuroinflammation. *Neuron*. 100:551-563 e557.
- 458 26. Dias C, Feng J, Sun H, Shao NY, Mazei-Robison MS, Dames-Werno D, et al. (2014):
459 beta-catenin mediates stress resilience through Dicer1/microRNA regulation. *Nature*.
460 516:51-55.

- 461 27. Bazargani N, Attwell D (2016): Astrocyte calcium signaling: the third wave. *Nature*
462 *neuroscience*. 19:182-189.
- 463 28. Khakh BS, McCarthy KD (2015): Astrocyte Calcium Signaling: From Observations to
464 Functions and the Challenges Therein. *Cold Spring Harbor Perspectives in Biology*. 7.
- 465 29. Ding F, O'Donnell J, Thrane AS, Zeppenfeld D, Kang H, Xie L, et al. (2013):
466 alpha1-Adrenergic receptors mediate coordinated Ca²⁺ signaling of cortical astrocytes in
467 awake, behaving mice. *Cell Calcium*. 54:387-394.
- 468 30. Anacker C, Luna VM, Stevens GS, Millette A, Shores R, Jimenez JC, et al. (2018):
469 Hippocampal neurogenesis confers stress resilience by inhibiting the ventral dentate
470 gyrus. *Nature*. 559:98-102.
- 471 31. Hultman R, Mague SD, Li Q, Katz BM, Michel N, Lin L, et al. (2016): Dysregulation of
472 Prefrontal Cortex-Mediated Slow-Evolving Limbic Dynamics Drives Stress-Induced
473 Emotional Pathology. *Neuron*. 91:439-452.
- 474 32. Dallerac G, Zapata J, Rouach N (2018): Versatile control of synaptic circuits by
475 astrocytes: where, when and how? *Nature reviews Neuroscience*. 19:729-743.
- 476 33. Hamilton NB, Attwell D (2010): Do astrocytes really exocytose neurotransmitters?
477 *Nature reviews Neuroscience*. 11:227-238.
- 478 34. Weikum ER, Knuesel MT, Ortlund EA, Yamamoto KR (2017): Glucocorticoid receptor
479 control of transcription: precision and plasticity via allostery. *Nature reviews Molecular cell*
480 *biology*. 18:159-174.
- 481 35. Bilanges B, Posor Y, Vanhaesebroeck B (2019): PI3K isoforms in cell signalling and
482 vesicle trafficking. *Nature reviews Molecular cell biology*. 20:515-534.

- 483 36. Zhang Z, Chen G, Zhou W, Song A, Xu T, Luo Q, et al. (2007): Regulated ATP
484 release from astrocytes through lysosome exocytosis. *Nat Cell Biol.* 9:945-953.
- 485 37. Williams EJ, Doherty P (1999): Evidence for and against a pivotal role of PI 3-kinase
486 in a neuronal cell survival pathway. *Molecular and cellular neurosciences.* 13:272-280.
- 487 38. Jia JM, Zhao J, Hu Z, Lindberg D, Li Z (2013): Age-dependent regulation of synaptic
488 connections by dopamine D2 receptors. *Nature neuroscience.* 16:1627-1636.
- 489 39. de Quervain D, Schwabe L, Roozendaal B (2017): Stress, glucocorticoids and
490 memory: implications for treating fear-related disorders. *Nature reviews Neuroscience.*
491 18:7-19.
- 492 40. Lupien SJ, McEwen BS, Gunnar MR, Heim C (2009): Effects of stress throughout the
493 lifespan on the brain, behaviour and cognition. *Nature reviews Neuroscience.* 10:434-445.
- 494 41. Holsboer F, Ising M (2010): Stress hormone regulation: biological role and translation
495 into therapy. *Annu Rev Psychol.* 61:81-109, C101-111.
- 496 42. McKlveen JM, Myers B, Flak JN, Bundzikova J, Solomon MB, Seroogy KB, et al.
497 (2013): Role of prefrontal cortex glucocorticoid receptors in stress and emotion. *Biological*
498 *psychiatry.* 74:672-679.
- 499 43. Barik J, Marti F, Morel C, Fernandez SP, Lanteri C, Godeheu G, et al. (2013): Chronic
500 stress triggers social aversion via glucocorticoid receptor in dopaminergic neurons.
501 *Science.* 339:332-335.
- 502 44. Tertilt M, Skupio U, Barut J, Dubovyk V, Wawrzczak-Bargiela A, Soltys Z, et al. (2018):
503 Glucocorticoid receptor signaling in astrocytes is required for aversive memory formation.
504 *Translational psychiatry.* 8:255.

- 505 45. Gururajan A, Reif A, Cryan JF, Slattery DA (2019): The future of rodent models in
506 depression research. *Nature reviews Neuroscience*. 20:686-701.
- 507 46. Wiktorowska L, Bilecki W, Tertilt M, Kudla L, Szumiec L, Mackowiak M, et al. (2021):
508 Knockdown of the astrocytic glucocorticoid receptor in the central nucleus of the
509 amygdala diminishes conditioned fear expression and anxiety. *Behavioural brain research*.
510 402:113095.
- 511 47. Pascual O, Casper KB, Kubera C, Zhang J, Revilla-Sanchez R, Sul JY, et al. (2005):
512 Astrocytic purinergic signaling coordinates synaptic networks. *Science*. 310:113-116.
- 513 48. Koyanagi S, Kusunose N, Taniguchi M, Akamine T, Kanado Y, Ozono Y, et al. (2016):
514 Glucocorticoid regulation of ATP release from spinal astrocytes underlies diurnal
515 exacerbation of neuropathic mechanical allodynia. *Nature communications*. 7:13102.
- 516 49. Cao X, Li LP, Qin XH, Li SJ, Zhang M, Wang Q, et al. (2013): Astrocytic adenosine
517 5'-triphosphate release regulates the proliferation of neural stem cells in the adult
518 hippocampus. *Stem Cells*. 31:1633-1643.
- 519 50. Iwata M, Ota KT, Li XY, Sakaue F, Li N, Dutheil S, et al. (2016): Psychological Stress
520 Activates the Inflammasome via Release of Adenosine Triphosphate and Stimulation of
521 the Purinergic Type 2X7 Receptor. *Biological psychiatry*. 80:12-22.
- 522 51. Miller AH, Raison CL (2016): The role of inflammation in depression: from
523 evolutionary imperative to modern treatment target. *Nat Rev Immunol*. 16:22-34.

524

525 **Figure legends**526 **Figure 1. The GR in astrocytes is more sensitive to stress than that in neurons. (A-B)**

527 Schematic of CSDS paradigm (A), and social interaction ratio of susceptible (Sus),
528 resilient (Res), and control (Ctrl) mice (B). **(C-D)** The GR protein in the mPFC of mice after
529 the CSDS (C) and correlated with social avoidance (D; $n = 7-8$ mice per group). **(E-F)**
530 Schematic representation of LPS-induced mouse model (E), and total immobility time of
531 mice treated with LPS in the FST (F; $n = 8$ mice per group). **(G-H)** The GR protein level in
532 the mPFC of adult C57BL/6J mice treated with LPS or saline (G) and correlated with
533 immobility time in the FST (H, $n = 6$ mice per group). **(I)**, Western blot analysis of the GR
534 protein in primary cultured astrocytes (DIV8) and neurons (DIV14) treated with LPS ($1\mu\text{g}$
535 ml^{-1}) or saline for 4 h ($n = 5-6$ per group). **(J-K)** Western blot analysis of the GR protein
536 level in primary cultured astrocytes (DIV8) and neurons (DIV14) exposed to
537 dexamethasone (DXMS; 0, 0.5, 1 and 5 μM) for 6 h (J; $n = 4$ per group) or DXMS (1 μM)
538 for 0, 4, 24 and 48 h (K; $n = 4$ per group). **(L)**, Representative images and quantification of
539 the co-expression of GR (red) and S100 β (green) in the mPFC of adult C57BL/6J mice (n
540 $= 6$ mice); Scale bars, 50 μm . **(M)** Representative images quantification of the
541 co-expression of GR (red) and NeuN (green) in the mPFC of adult C57BL/6J mice ($n = 6$
542 mice); Scale bars, 50 μm . Data are the mean \pm s.e.m. * $P < 0.05$, ** $P < 0.01$, *** $P < 0.001$.
543 Two-tailed unpaired t -test (**F, G, I, L, M**), one-way ANOVA followed by Bonferroni's
544 multiple comparison test (**B, C, J, K**), and correlations were evaluated with Pearson's
545 correlation coefficient (**D, H**).

546 **Figure 2. Astrocyte-specific loss of GRs displays depressive- and anxiety-like**
547 **behaviors. (A)** Genetic crosses used to delete astrocytic GRs from the whole brain and
548 experimental design of behavioral studies. PND, postnatal day. **(B)** Flow cytometry

549 analysis of the GR expression in astrocytes from cKO and Ctrl mice 28 days after
550 tamoxifen induction. The gray line depicts unstained control, black and red line GR
551 staining, and numbers indicate the percentage of GR-positive astrocytes. **(C)**
552 Quantification of GR-positive astrocytes of cKO and Ctrl mice (n = 3 mice per group). **(D)**
553 Total immobility time in the FST (n = 11,14 mice). **(E)** Representative heatmaps and
554 quantification of time spent in the interaction zone before and after SSDS (n = 9, 13 mice).
555 **(F)** Time spent in the open arms and closed arms in the EPM (n =11, 15 mice). **(G)** Time
556 spent in the dark box in the LD box (n = 12,15 mice). **(H-I)** Total distance (H) and center
557 time (I) for cKO and Ctrl mice in the open field test (n = 13, 15 mice). **(J)** Latency to fall of
558 cKO and Ctrl mice in the rotarod test (n = 11,13 mice). Data are the mean \pm s.e.m. **P* <
559 0.05, ***P* < 0.01, ****P* < 0.001. Two-tailed unpaired *t*-test **(C, D, F, G, H, I)** and matching
560 two-way ANOVA followed by Bonferroni's multiple comparison test **(E, J)**.

561 **Figure 3. Astrocytic GRs in the mPFC modulate depressive-like behaviors. (A)**
562 Experimental design of behavioral studies of *Nr3c1^{loxP/loxP}* mice infected with
563 AAV-GFAP-CRE virus. **(B)** Representative images of AAV-GFAP-CRE expression in the
564 mPFC of *Nr3c1^{loxP/loxP}* mice. Scale bars, 500 μ m (left), 50 μ m (right). **(C)** Western blot
565 analysis of GRs in the mPFC in different groups (n = 5 mice per group). **(D)** Total
566 immobility time in the FST (n = 11, 12 mice). **E**, Social avoidance behaviors before and
567 after SSDS (n = 9 mice per group). **(F)** Time spent in the open and closed arms for the
568 control and Cre in the EPM test (n = 11, 12 mice). **(G-H)** Total distance (G) and center
569 time (H) for Cre and control mice in the open field test (n = 11, 12 mice). **(I)** Representative
570 images of AAV-Ef α 1-DIO-Nr3c1-3xFlag expression in the mPFC of cKO mice. Scale bars,

571 500 μm (left), 50 μm (right). **(J)** The social avoidance behaviors of cKO and Ctrl mice
572 before and after SSDS ($n = 10$ mice for Ctrl+EYFP and Ctrl+GR; $n = 11$ mice for
573 cKO+EYFP; $n = 12$ mice for cKO+GR). **(K-L)** Total distance (K) and center time (L) for Ctrl
574 and cKO mice infected with AAV-Ef α 1-DIO-Nr3c1-3xFlag or control virus ($n = 8$ mice per
575 group). Data are the mean \pm s.e.m. * $P < 0.05$, ** $P < 0.01$, N.S. not significant. Two-tailed
576 unpaired t-test (**C, D, F, G, H**), one-way (**K, L**), and matching two-way ANOVA followed by
577 Bonferroni's multiple comparison test (**E, J**).

578 **Fig. 4. The GR deletion decreases astrocytic Ca²⁺ activity in the mPFC. (A)**

579 Experimental design of fiber photometry. **(B)** Schematic illustrating fiber placement and
580 representative images of GCamp6s expression. Scale bars, 500 μm (left), 50 μm (right).
581 **(C)** Representative heatmaps of GCaMP6s transient z-scores event-locked to social
582 interaction. Each row plots one trial and a total of 4 trials are illustrated. **(D-E)** Average (D)
583 and peak (E) z-score changes during social interaction ($n = 4$ mice per group). Data are
584 the mean \pm s.e.m. * $P < 0.05$. Matching two-way ANOVA followed by Bonferroni's multiple
585 comparison test (**E**).

586 **Figure 5. GRs modulate astrocytic ATP release in the mPFC. (A)** The concentration of

587 plasma corticosterone in cKO and Ctrl mice under basal conditions or after an additional
588 acute social defeat episode ($n = 6-8$ mice per group). **(B)** Measurements of
589 neurotransmitter levels (aspartate (Asp), glutamate (Glu), serine (Ser), glutamine (Gln),
590 glycine (Gly), GABA, and ATP) in the medium of slices of the PFC ($n = 5-8$ mice). **(C)** In
591 vivo microdialysis in freely moving mice showing ATP levels in the mPFC ($n = 8$ mice per
592 group). **(D-E)** ATP levels in the medium of primary cultured astrocytes (D, $n = 6$) and

593 GR-knockdown astrocytes (E, n = 6) treated with DXMS or vehicle for 4 h. **(F)**
594 Experimental design of fiber photometry. **(G)** Schematic illustrating fiber placement and
595 representative images of AAV-GfaABC1D-ATP1.0 expression. Scale bars, 500 μm (left),
596 50 μm (right). **(H)** Representative heatmaps of ATP1.0 transient z-scores event-locked to
597 social interaction. Each row plots one trial and a total of 4 trials are illustrated. **(I-J)**
598 Average (I) and peak (J) z-score during social interaction (n = 4 mice per group). **(K)**
599 Experimental design of ATP treatment. **(L)** Total immobility time in the FST (n = 9-12
600 mice). Data are the mean \pm s.e.m. * $P < 0.05$, ** $P < 0.01$, *** $P < 0.001$. Two-tailed unpaired
601 t-test **(B)**, two-tailed paired t-test **(C)**, one-way ANOVA followed by Bonferroni's multiple
602 comparison test **(D, L)**, two-way ANOVA followed by Bonferroni's multiple comparison test
603 **(A, E, J)**.

604 **Fig. 6. The PI3K-AKT signaling pathway mediates GR-dependent astrocytic ATP**
605 **release. (A)** Volcano plot of the differentially expressed genes (DEGs) between cKO and
606 Ctrl astrocytes isolated from the mPFC (n = 3 independent biological samples per group).
607 **(B)** Hierarchical clustering based on the expression profiles of DEGs. **(C)** Enriched KEGG
608 pathways. **(D)** Western blot analysis of p-PI3K, PI3K, p-AKT, and AKT protein levels in
609 cultured astrocytes after 4 h of DXMS (1 μM) or vehicle treatment (n = 5). **(E)** ATP levels
610 in the medium of cultured astrocytes treated with DXMS (1 μM) or vehicle for 4 h in the
611 presence or absence of the PI3K inhibitor LY29004 (40 μM) (n = 5-6). **(F)** Effects of GPN
612 (200 μM) on the DXMS-induced release of ATP from astrocytes (n = 5-6). **(G)** Confocal
613 fluorescent images of LysoTracker uptake in living astrocytes treated with 740-YP (50 μg
614 ml^{-1}) and vehicle for 4 h. Scale bar, 20 μm . **(H)** The mean fluorescence intensity of

615 Lysotracker was quantified using ImageJ (n = 6 separate experiments). **(I)** Confocal
616 fluorescent images of Lamp1 in astrocytes treated with 740-YP (50 $\mu\text{g ml}^{-1}$) or vehicle for
617 4 h. Scale bar, 10 μm . **(J)** The number of lysosomes per 100 μm^2 in 19 and 18 astrocytes
618 treated with vehicle or 740-YP, respectively. **(K)** Distribution of the lysosome surface (μm^2).
619 1136 and 1214 lysosomes were measured in astrocytes treated with vehicle or 740-YP,
620 respectively. The lysosomal size was ranged from 0.01 to 1 μm^2 . χ^2 test of independence:
621 $\chi^2 = 2.419$, df 10, $P = 0.992$. **(L)** A model for mechanisms of depression indicated that the
622 GR-dependent astrocytes mediated stress vulnerability in mice. Temporal elevations in
623 glucocorticoid levels preferentially activated astrocytic GRs, thereby enhancing
624 extracellular ATP release through lysosome exocytosis. ATP released from astrocytes
625 bound to purinergic receptors on neurons. Chronic stress induced a reduction of astrocytic
626 GRs in the mPFC, which consequently decreased ATP released from astrocytes to
627 regulate depressive-like behaviors. Data are the mean \pm s.e.m. * $P < 0.05$, ** $P < 0.01$,
628 *** $P < 0.001$, N.S., not significant. Two-tailed unpaired t-test **(D, H, J)** and one-way
629 ANOVA followed by Bonferroni's multiple comparison test **(E, F)**.

